Methodology to assess the impact of electrochemical model parameters based on design of experiments

L. Oca[1,*], E. Miguel[1], L. Otaegui[2], A. Villaverde[2], U. Iraola[1]

[1] Mondragon Unibertsitatea, Electronic and computing department, Loramendi 4, Mondragon 20500, Basque Country, Spain.

[2] CIC energiGUNE, Arabako Teknologi Parkea, Albert Einstein 48, Miñano 01510, Spain

[*]lauraoca@mondragon.edu

Abstract: Electrochemical models are a key factor in the development and optimization of actual and new energy storage devices. The aim of this work is to present a new tool for optimization of the internal parameters of the cells by means of electrochemical models and design of experiments. For the validation of this methodology, Doyle cell parameters have been used. A two-level full factorial design of 9 design parameters has been evaluated to identify the significant parameters. 8 factors have resulted to be significant, so a three-level full factorial design has been performed to apply the response surface methodology. Finally, an optimization based on Nelder-Mead simplex algorithm has been used to maximize the aggregate desirability function. In this paper, it is demonstrated that the use of design of experiments coupled with electrochemical battery models are suitable for the optimization of the design parameters of the cell.

Keywords: design of experiments, electrochemical model, battery, P2D model.

1. Introduction

Energy storage devices should be enhanced to cope with the energy and power density requirements of different applications [1]. In order to achieve that objective, electrochemical models can be used. They can provide useful information related to the internal mechanisms of the batteries which can help in the development and redesign of existing Li-ion batteries. Moreover, they can aid to develop more innovative concepts [2].

The aim of this work is to present a new tool for optimization of the internal parameters of the cells by means of electrochemical models and design of experiments. In order to cope with that objective, the paper has been divided in three main sections. First of all, the model framework and the analysed cell is presented. In the second section, the applied methodology is explained, which covers four steps: the design of experiments (DOE) definition, the electrochemical model solving, the post-processing of the results and cell optimization. In the last section the results obtained with the Doyle cell [3] with this methodology are presented.

2. Model description

A physics-based battery model implemented in COMSOL Multiphysics® simulation software and developed by G. Plett *et. al.* [2] is used for the analysis. This model is based on the mathematical framework developed by Newman *et. al.*[4]. The geometry, governing equations, boundary conditions and parameters are briefly described in this section according to [2 - 6]. This continuum model consist on a 1-D macroscopic model coupled with a pseudo dimension that is represented in the Figure 1 (P2D model).

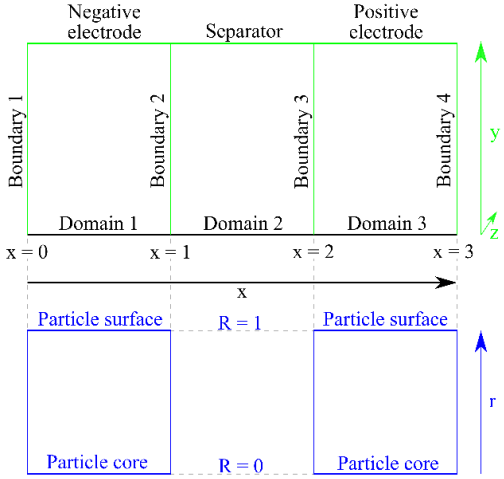

Figure 1. Schematic representation of the electrochemical model. Blue color represents the pseudo-dimension (*r*) in which a particle is presented. Black color represents the 1D dimension (*x*) of the model, thicknesses of the components of the cell (3 domains and 4 boundaries). Green color represents *y* and *z* dimensions that are used to calculate the cross-sectional area (A = 1 m^2).

The macroscopic model consists of three domains: a negative electrode, a separator and a positive electrode (see Figure 1). There are four boundaries. The first and fourth boundaries correspond to the interface between the electrode and the current collectors, while the second and third boundaries are the interfaces between the electrodes and separator.

The macroscopic description of this model is defined by volume averaging over small finite volume units of microscopic quantities. In that approach, the electrodes are considered as the superposition of two continua, representing the solid and the liquid phases. Moreover, the electrodes are considered as porous matrixes of electrochemically reactive and electrically conductive solids. The model assumes that the electrolytic solution completely fills the voids of the porous solid matrix. This means that solid and liquid matrixes are considered separately.

The microscopic model describes the active material particles and is represented in a pseudo-dimension (see Figure 1). In this pseudo-dimension, each electrode has one domain and two boundaries in which R = 0 corresponds to the particle core and R = 1 to the particle surface. Microscale geometries are described assuming volume-averaging theorems.

2.1. Governing equations and boundary conditions

The model is composed of a set of four partial-differential equations (PDE's) and one algebraic equation. These equations describe the dynamics of a cell. The PDE's solve the charge and material balance in the liquid and solid-phases. Those equations are coupled with the pore wall flux algebraic equation. The model solves the spatial and time evolution of five variables: the potential and the lithium concentration of the solid particles, the potential and lithium ion concentration in the electrolyte and the flux of lithium ions out of a particle. In the following lines, the governing equations and its boundary conditions are presented.

The first PDE is related to the charge conservation in the solid-phase. This equation is derived from Ohm's law (eq. 1):

$$\frac{\partial}{\partial x}\left(\sigma_{eff}\frac{\partial}{\partial x}\phi_s(x,t)\right)-a_s F j(x,t)=0 \qquad (1)$$

where ϕ_s is the solid-state potential in the electrodes.

The applied boundary conditions for the current conservation of the solid-phase are presented in eq. 2:

$$\sigma_{eff}^{pos}\frac{\partial}{\partial x}\phi_s(3,t)=-\sigma_{eff}^{neg}\frac{\partial}{\partial x}\phi_s(0,t)=\frac{i_{app}}{A} \qquad (2)$$

where x = 0 starts from the negative current collector (boundary 1 in Figure 1) and x = 3 represents the positive current collector(boundary 4 in Figure 1).

The second PDE is linked to the charge conservation in the liquid-phase, which is modelled using Ohm's law (eq. 3):

$$\frac{\partial}{\partial x}\left(\kappa_{eff}\frac{\partial}{\partial x}\phi_e(x,t)\right)+a_s F j(x,t)+ \\ +\frac{\partial}{\partial x}\left(\kappa_{D,eff}\frac{\partial}{\partial x}\ln(c_e(x,t))\right)=0 \qquad (3)$$

where ϕ_e is the liquid-phase potential.

The boundary conditions of ϕ_e are,

$$\kappa_{eff}\frac{\partial}{\partial x}\phi_e(0,t)+\kappa_{D,eff}\frac{\partial}{\partial x}\ln(c_e(0,t))=0 \\ \kappa_{eff}\frac{\partial}{\partial x}\phi_e(3,t)+\kappa_{D,eff}\frac{\partial}{\partial x}\ln(c_e(3,t))=0 \qquad (4).$$

The third PDE is the material balance of the electrolyte and it is described in eq. 5,

$$\frac{\partial(\varepsilon_e c_e(x,t))}{\partial t}=\frac{\partial}{\partial x}(D_{e,eff}\frac{\partial}{\partial x}c_e(x,t))+ \\ +a_s(1-t_+^0)j(x,t) \qquad (5)$$

where c_e is the $LiPF_6$ salt concentration.

The boundary conditions applied for the material balance are:

$$\frac{\partial(c_{e,ratio}(0,t))}{\partial x}=\frac{\partial(c_{e,ratio}(3,t))}{\partial x}=0 \qquad (6).$$

The last PDE models the pseudo-dimension (r) of the continuum model. The equation is derived from Fick's law of diffusion for spherical particles:

$$\frac{\partial c_s(r,x,t)}{\partial t}=\frac{D_s}{r^2}\frac{\partial}{\partial r}\left(r^2\frac{\partial c_s(r,x,t)}{\partial r}\right) \qquad (7)$$

where c_s is the solid-state Li^+ ions concentration.

The applied boundary conditions are:

$$D_s \frac{\partial c_s(0,x,t)}{\partial r} = 0$$
$$t \geq 0 \qquad (8).$$
$$D_s \frac{\partial c_s(R_s,x,t)}{\partial r} = -j(x,t)$$

Finally, the pore wall flux of Li^+ ions in the electrodes (j) is described by the Butler-Volmer kinetics equation (eq. 9).

$$j = \kappa_{0,norm}\left(\frac{c_e}{c_{e,0}}\right)^{1-\alpha}\left(\frac{c_{s,\max}-c_{s,e}}{c_{c,\max}}\right)^{1-\alpha}\left(\frac{c_{s,e}}{c_{s,\max}}\right)^{\alpha} \left\{\exp\left(\frac{(1-\alpha)F}{RT}\eta\right)-\exp\left(\frac{\alpha F}{RT}\eta\right)\right\} \qquad (9)$$

Where the local surface overpotencial η is defined as:

$$\eta = \phi_s - \phi_e - U_{ocp}(c_s) - FR_{film}\, j \qquad (10).$$

2.2. Analysed system

The cell is composed of Carbon and Lithium Manganese Oxide (LMO) electrodes and the electrolyte is a mixture of lithium hexafluorophosphate salt ($LiPF_6$) and commonly used organic carbonate solvents (Ethylene Carbonate (EC) and Dimethyl Carbonate (DMC)). The cell parameters used for the validation of this methodology are taken from Doyle et. al. [3] and are summarized in Table 1 and 2.

Table 1. Electrode parameters (25 ºC).

Parameter	Description	Negative electrode	Positive electrode
D_s (m^2 s)	Solid diffusion	$3.9\ 10^{-14}$	$1.0\ 10^{-13}$
σ (S m^{-1})	Electric conductivity	100	3.8
$c_{s,max}$ (mol m^3)	Maximum Lithium concentration	26390	22860
$c_{s,0}$ (mol m^3)	Initial lithium concentration	14870	3900
L (m)	Thickness	$1.28\ 10^{-4}$	$1.9\ 10^{-4}$
R_s (m)	Particle radius	$12.5\ 10^{-6}$	$8.5\ 10^{-6}$
ε_e (-)	Liquid volume fraction	0.357	0.444
ε_s (-)	Solid volume fraction	0.471	0.297
brug	Bruggeman coefficient	1.5	1.5
k (mol m^{-2} s^{-1})	Reaction rate	$2.29\ 10^{-5}$	$2.21\ 10^{-5}$
R_{film} (Ω)	Film resistance	0.03	0

Table 2. Separator and electrolyte parameters (25 ºC).

Parameter	Description	Separator	Electrolyte
L (m)	Thickness	$0.76\ 10^{-4}$	
ε_s (-)	Solid volume fraction	0.724	
$\kappa_{ref,0}$ (S m^{-1})	Initial conductivity		0.105
brug	Bruggeman coefficient	1.5	
α	Transfer coefficient		0.5
D_e (m^2 s)	Diffusion coefficient		$7.5\ 10^{-11}$
t_+	Transport number		0.363
$c_{e,0}$ (mol m^3)	Initial concentratior		2000

* D_e and $c_{e,0}$ has been changed from the Doyle cell which original values were $7.5\ 10^{-7}$ (m^2 s) and 1000 (mol m^3) respectively.

3. Applied methodology

In the present study, a methodology based on design of experiments (DOE) is proposed to evaluate the response of a cell when design parameters are changed. The objective is to balance the major limitations of the cell, to reach the optimal design in the analysed range. The full procedure implemented in this work is shown in Figure 2 and explained in the next subsections.

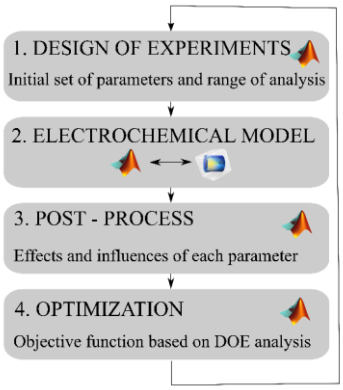

Figure 2. Methodology overview.

3.1. Design of experiments applied to simulations

The design of experiments is widely used to analyse the effects and interactions of a certain number of design parameters (**factors**) on pre-defined outputs (**responses**) [7]. This method can be used to determine the minimum set of experiments needed to reach to an optimal design. The DOE consist of varying one design parameter of the cell to

assess individual effects (**main effects**) and analyses interactive effects (**interaction effects**) between the selected design parameters. Interaction effects represent how a response is affected by more than one parameters. A main effect represents how a single parameter affects in the analysed. Nevertheless, that response is usually affected by other parameters, and the results can be badly interpreted. That is why interaction effects are also important to be analysed.

In this study, a two-level full factorial design (FFD) with 9 factors is proposed to evaluate if all these factors are significant to the evaluated responses. Moreover, a three-level full factorial design is used to apply the **surface response methodology** (SRM). In the Table 3 the analysed design parameters and the high and low values selected for those factors are presented.

Table 3. Parameter range of the two-level FFD.

Parameter	Low (-1)	High (+1)
$L_{\_neg}$ (m)	$1.28\ 10^{-4}$	$1.54\ 10^{-4}$
m_r(-)	0.49	0.59
ε_{s_neg} (-)	0.471	0.57
ε_{s_pos} (-)	0.297	0.36
$R_{s,neg}$ (m)	$12.5\ 10^{-6}$	$15\ 10^{-6}$
$R_{s,pos}$ (m)	$8.5\ 10^{-6}$	$10.2\ 10^{-6}$
σ_{neg} (S m^{-1})	100	120
σ_{pos} (S m^{-1})	3.8	4.6
$c_{e,0}$ (mol m^3)	2000	2400

* neg and pos denote the positive and negative electrodes respectively and m_r is the mass balance of the cell.

For the two-level full factorial design, the low level value corresponds to the Doyle value. The high level value was calculated as a 20% increase with respect to the low level value. The 20 % increase has been arbitrarily selected as a compromise between detecting a significant change in the response but maintaining its linearity. Further experiments are planned to be done in future works to select the correct range of variation for each parameter. This percentage could significantly affect the obtained results of the study [8]. All in all, in this work, the validity of the applied methodology is discussed so further studies will be performed after the validation of the tool. The mean value of the analysed range has also been included in the three-level full factorial design performed in order to apply the response surface methodology.

The first 6 factors of the analysis have been selected as they can be varied during the manufacturing process of the batteries. The negative electrode thickness and mass ratio between electrodes are common parameters that need to be defined in the manufacturing process. Moreover, the electric conductivity of the electrodes has been analysed. This variation could be found in a real scenario decreasing the carbon content of the electrodes or with different doping strategies [9]. Finally, the electrolyte initial concentration has been changed to determine the transport limitations of the cell. Note that the electrolyte conductivity varies as a function of the electrolyte concentration.

In addition to these 9 factors, there are three parameters (positive electrode thickness, liquid volume fraction and specific surface area) that need to be re-calculated depending on the factor level.

The positive electrode thickness can be calculated with the mass balance of the cell:

$$m_r = \frac{m^{neg}}{m^{pos}} = \frac{A\rho^{neg}L^{neg}(1-\varepsilon_e^{neg}-\varepsilon_{b+a}^{neg})}{A\rho^{pos}L^{pos}(1-\varepsilon_e^{pos}-\varepsilon_{b+a}^{pos})} \qquad (11),$$

where ρ^{pos} and ρ^{neg} are the solid phase density of the positive and negative electrode which are 4140 and 1900 kg m^{-3} respectively [3].

The liquid volume fraction is calculated from eq. 12, as the total volume of the electrode is the unity.

$$\varepsilon_s + \varepsilon_e + \varepsilon_{b+a} = 1 \qquad (12),$$

$\varepsilon_{a,b}$ corresponds to the solid volume fraction of the additives and binder which are 0.172 and 0.259 in the negative and the positive electrode respectively [3].

Finally, the specific surface area is calculated assuming that the electrodes are made of spherical particles of uniform size and distribution.

$$a_s = \frac{3\varepsilon_s}{R_s} \qquad (13).$$

In this paper, energy and power density (E_m and P_m) responses have been analysed. Solving the electrochemical model

The model explained in section two is solved using COMSOL Multiphysics® software linked with the LiveLink™ for MATLAB®. A HP Z840 Workstation has been used in order to speed up the computation time using parallel computing. In this case, 20 workers have been employed in every batch of simulations.

3.2. Post-processing of the results

In this work, 5C galvanostatic discharge process and 1C charge process have been selected to evaluate the cell. The selected current rates represent the

maximum rate of each process, based on Doyle *et. al.* work [3]. The two-level full factorial design with 9 factors has been post-processed in MATLAB® in order to build a linear regression model for each analysed response and identify the meaningful factors and interactions. Once the meaningful factors are identified, a three-level full factorial design of the relevant factors has been evaluated via response surface methodology.

3.3. Model optimization

The desirability function approach has been used to transform each output response into a 0 to 1 response in order to perform the maximization of the aggregate desirability value. A Nelder-Mead based algorithm has been used for optimization. As the optimization is based on regression models, the accuracy of the predicted values is not as accurate as the ones obtained with the electrochemical model. Therefore, to conclude the analysis, the optimized design factors are run in COMSOL Multiphysics® software and the results are compared with the Doyle cell (reference cell).

4. Results and discussion

This section has been divided in three parts: the two and three full factorial design analysis and the verification of the optimized results.

4.1. Two-level full factorial design

The results obtained for the energy density of the two-level full factorial design are shown. The same methodology has been applied for the power density response, although only E_m graphs are shown. In the optimization routine both responses are used. In Figure 3, the half probability plot of the energy density is presented. The factors that are far from the straight line are considered significant for a particular response, whereas the rest are considered not meaningful.

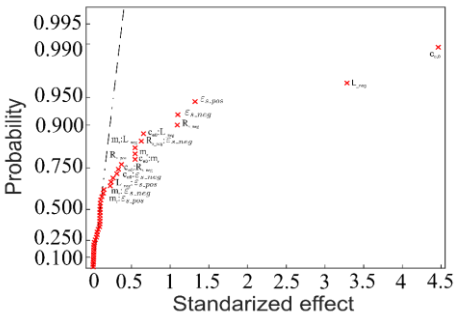

Figure 3. Half probability plot for the E_m response.

Moreover, a linear model using stepwise regression has been built. For this model, non significant parameters are removed (p-value < 0.05). Interactions up to first order have been analysed. In the following equation, an example of the linear regression model for the energy density is shown. The root mean square (RMS) value of the model is 0.892. The results presented in Figure 3 and the linear regression are in good concordance.

$$E_m = -49.60 + 0.02\,c_{e,0} + 127\,m_r + 75.7910^4\,L_{\_neg} - 69.2810^4\,R_{s\_neg} - 148.97\,\varepsilon_{s\_neg} + 19.5210^4\,R_{s\_pos} + 68.09\,\varepsilon_{s\_pos} - 0.03\,c_{e,0}\,m_r - 128.02\,c_{e,0}\,L_{\_neg} - 741.78\,c_{e,0}\,R_{s\_neg} + 0.02\,c_{e,0}\,\varepsilon_{s\_neg} - 43.5910^4\,m_r\,L_{\_neg} - 51.33\,m_r\,\varepsilon_{s\_neg} - 77.34\,m_r\,\varepsilon_{s\_pos} - 34.5410^4\,L_{\_neg}\,\varepsilon_{s\_pos} + 53.3110^4\,R_{s\_neg}\,\varepsilon_{s\_neg} \quad (14).$$

In the Figure 4 the main effect of the energy density response is presented. In this case, only the positive active material particle radius is a main effect, as the remaining are treated as an interaction. It is possible to conclude that a slightly higher value of positive active material radius could improves the energy density of the cell.

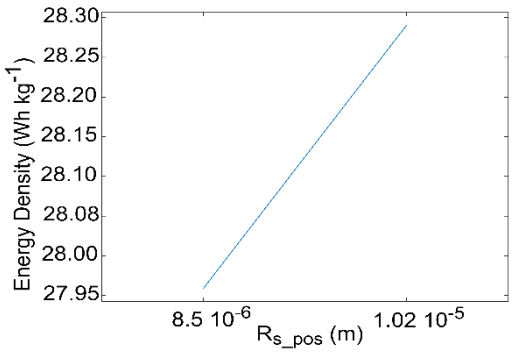

Figure 4. Main effects for the energy density response.

The interactions between parameters are shown in Figure 5. In all the cases, the low parameter level of the initial concentration of the electrolyte improves the energy density. In addition to this, a decrease in the solid volume fraction of both electrodes could be beneficial in terms of energy density. Moreover, increasing the negative electrode thickness and a slight increase of the negative particle radius increases the target. The high level value of the mass ratio seems to give slightly higher results in energy density.

For all the analysed responses, the electric conductivity of the negative electrode is not significant in this analysed range. Therefore, in the three-level full factorial design that factor has been removed. Note that in the energy density response, the electric conductivity of the positive electrode is

not significant, but it is significant within the analysed responses. Further analysis should be done in other design parameter range to see the effect of electric conductivity in the overall cell response.

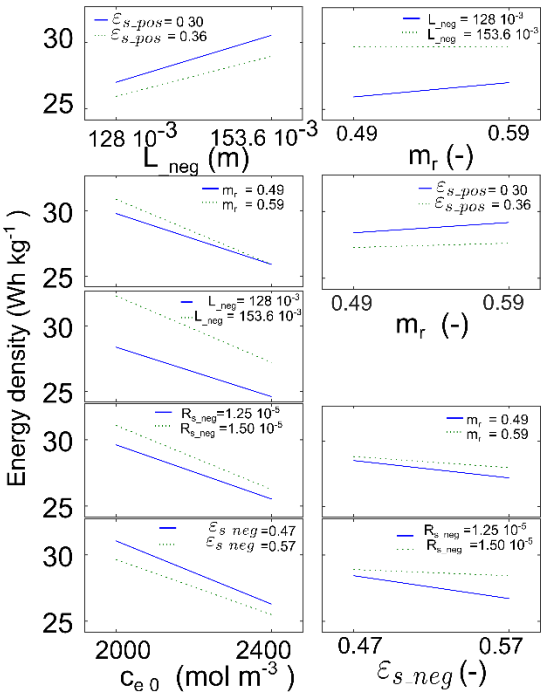

Figure 5. Interactions for the energy density response.

4.2. Three-level full factorial design

The response surface methodology has been used to establish a relationship between the two responses (E_m and P_m)and the design factors. A second degree model is commonly used for this purpose [10].

$$y = \beta_0 + \sum_{i=1}^{k} \beta_i x_i + \sum \sum_{i<j} \beta_{ij} x_i x_j + \sum_{i=1}^{k} \beta_{ii} x_i^2 + error \quad (15),$$

where y is the response, x_i are the design factors, k is the number of factors, β terms correspond to the fitting coefficients.

In order to collect the necessary data for the RSM, central composite design (CCD), 3^k full factorial factorial design and box-behkin design (BBD) matrices are normally used [10]. In this work, a three-level full factorial model has been selected with 8 significant factors (electric conductivity of negative electrode has been removed due to the results obtained in the 2^k FFD). The used range of parameters are presented in Table 4.

Table 4. Parameter values for three-level FFD.

Parameter	Low (-1)	Mean (0)	High (+1)
$L_{\_neg}$ (m)	$1.28\ 10^{-4}$	$1.41\ 10^{-4}$	$1.54\ 10^{-4}$
m_r(-)	0.49	0.54	0.59
ε_{s_neg} (-)	0.471	0.518	0.57
ε_{s_pos} (-)	0.297	0.327	0.36
$R_{s,neg}$ (m)	$12.5\ 10^{-6}$	$13.8\ 10^{-6}$	$15\ 10^{-6}$
$R_{s,pos}$ (m)	$8.5\ 10^{-6}$	$9.35\ 10^{-6}$	$10.2\ 10^{-6}$
σ_{pos} (S m^{-1})	3.8	4.2	4.6
$c_{e,0}$ (mol m^3)	2000	2200	2400

In the Figure 6 the most significant design factor interaction of the energy density is presented. Between the significant interactions (p_value < 0.05) only the strongest one (high F-value) has been plotted. The R^2 of the model is 0.996.

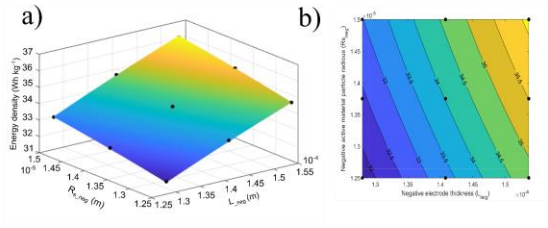

Figure 6. a) 3D surface plot and b) contour plot for the most significant interaction for the energy density (E_m).

4.3. Output response optimization

In the previous subsection, each response have been analysed separately. However, in order to reach an optimal design, the output responses should be analysed together. First of all, each output response (y_i) is transformed into one desirability function $d_i(y_i)$, in order to have a comparable magnitude that goes from zero to one [10]. The desirability function is calculated as:

$$d_1[y_1(x)] = \begin{cases} 0 & if\ y_i(x) < L_i \\ \left(\dfrac{y_i(x) - L_i}{U_i - L_i}\right)^r & if\ L_i \le y_i(x) \le U_i \\ 1 & if\ y_i(x) > U_i \end{cases} \quad (16)$$

where L_i and U_i are the low and up values of the response and r is a weight factor.

The objective function is built as:

$$D(d_1[y_1(x)], d_2[y_2(x)]..., d_n[y_n(x)]) = \left(\prod_{i=1}^{n} d_i[y_n(x)]\right)^{1/n} \quad (17),$$

where D is the aggregate desirability value.

For this specific example, energy and power density responses have been maximized together. The limit values of the responses are E_m (24 – 38) and P_m (340 – 420). Those boundary values have been selected based in the range of analysis obtained in the simulations. Finally, a Nelder-Mead simplex algorithm has been used in which the desirability function is maximized. Optimized values are displayed in Table 5:

Table 5. Optimized design factors for E_m/P_m responses.

L_{neg}	m_r	ε_{s_neg}	ε_{s_pos}
1.28 e^{-4}	0.51	0.47	0.32
$R_{s,neg}$	$R_{s,pos}$	σ_{pos}	$c_{e,0}$
1.26 e^{-5}	8.57 e^{-6}	3.84	2117

4.4. Validation of the optimized design factors

The optimized values obtained in this work compared to the reference simulation are shown in Table 6. An increase in the power density of the cell is obtained with a slight decrease in the energy density. The minimum electrolyte concentration of the cell is slightly higher. The minimum solid concentration of the electrodes does not change drastically, as the analysed range is not wide. Although in the negative electrode the minimum value is higher, it might be due to the extra lithium content of the electrolyte in that region that improves the discharge process at high rates (Initial lithium concentration in the electrolyte has increased from 2000 to 2117 mol m^{-3}).

Table 6. Reference and optimized responses.

Response	Doyle cell	Optimized cell
ce_min	696	713
$c_{s\_neg,min}$	1435	1467
$c_{s\_pos,min}$	1832	1795
E_m	32	31
P_m	396	408

Depending on the optimization objective, different design parameter configurations are obtained. However, with the increase of the number of parameters and responses to analyse, the optimization results are less accurate, as there is a wide range of combinations.

5. Conclusions and future lines

This paper presents a proof of concept for the optimization of the design parameters of batteries using the design of experiments. It has been demonstrated that the use of the presented methodology is suitable for the optimization of the design parameters of the cell in a specific range and for specific responses of the model. This methodology can be applied to evaluate and improve the performance of real cells in which internal parameters are experimentally obtained using the most suitable characterization techniques. In addition, this tool can help in the design of new cells, as it provides highly valuable insights on the response of the internal variables as a function of design parameters.

In future studies the full range of parameters need to be analysed in order to find the global optimum. In this paper, the results represents a local optimum, since only the 20 % of parameter variation has been analysed. In addition, only galvanostatic charge/discharge processes have been analysed. It should be taken into account other cycling regimes such us pulses, to get a deeper insight of the cell dynamics. Moreover, different responses of the model can be analysed, such as, minimum concentration of the electrolyte in the whole cell (c_{e_min}) and minimum solid concentration in both electrodes ($c_{s\_neg,min}$ and $c_{s\_pos,min}$) will be analysed. Moreover, a central composite design (CCD) or box-behkin design (BBD) could be used instead of 3^k factorial design as a way to reduce the computation time of the whole methodology.

6. References

[1] G. Jeong *et.al.*, *Energy Environ. Sci.*, **4** (6), 1986–2002 (2011).
[2] G. Plett, *Battery Management Systems: Battery modeling, Volume I.* Artech House (2015).
[3] M. Doyle *et. al.*, *J. Electrochem. Soc.*, **143** (6)1890–1903 (1996).
[4] M. Doyle *et. al.*, *J. Electrochem. Soc.*, **140** (6), 1526–1533 (1993).
[5] J. Newman and W. Tiedemann, *AIChE J.*, **21** (1), 25–41 (1975).
[6] T. F. Fuller, *J. Electrochem. Soc.*, **141** (1), 1 (1994).
[7] J. Antony, *Design of Experiments for Engineers and Scientists*. Butterworth Heinemann (2003).
[8] Z. He and E. T. M. Dass, *Appl. Math. Model.*, **57** 656–669 (2018).
[9] F. Jiang and P. Peng, *Sci. Rep.*, **6**, no. August, pp. 1–18, 2016.
[10] S. Younis *et. al.*, *Microelectronics J.*, **71**, 47–60 (2018).

Acknowledgements

Authors would like to thank G. Plett and S. Trimboli for sharing their electrochemical model and knowledge. Authors gratefully acknowledge financial support of the Basque Government for the project KK-2017/00066 funded by ELKARTEK 2017 programme and the predoctoral grant (PRE.2018.2.0117).